IAES International Journal of Artificial Intelligence (IJ-AI)
Vol. 15, No. 6, December 2026, pp. 5408~5417
ISSN: 2252-8938, DOI: 10.11591/ijai.v15.i6.pp5408-5417

Enhanced blood cancer diagnosis using swin U-net transformer segmentation and hybrid feature-based classification

Shenbagarajan Anantharajan[1], Shenbagalakshmi Gunasekaran[2], Sivaganesh Anantharajan[3], Thavasi Subramanian[2]
[1]Department of Artificial Intelligence and Data Science, Mepco Schlenk Engineering College, Sivakasi, India
[2]Department of Computer Science and Engineering, Mepco Schlenk Engineering College, Sivakasi, India
[3]Master of Computer Application, Mepco Schlenk Engineering College, Sivakasi, India

Article Info

Article history:

Received Jul 13, 2025
Revised Aug 8, 2026
Accepted Aug 31, 2026

Keywords:

Blood cancer
CLAHE
Histopathological images
Local binary patterns
Swin UNETR

ABSTRACT

Early diagnosis is required for diagnosing blood cancer properly. Every year, 6,000 cases of cancer are reported worldwide owing to this condition. This system proposes an advanced and automated way of detecting and classifying blood cancer by utilizing deep learning and machine learning algorithms. The first step in the process involves resizing, normalization and contrast-limited adaptive histogram equalization (CLAHE) enhancement of the histopathological images. The swin U-net transformer (UNETR) model which uses transformers, is used to accurately separate cancerous areas from preprocessed images. Both local binary patterns (LBP) and an adaptive threshold directional binary gradient (AT-DBGM) are used to extract features which include both local and global information. The features are passed one after another to add more detail and then an XGBoost model is used to classify the different stages of blood cancer. The system is designed to group input images into four groups: benign, early, proliferative, and pre-leukemic. This work achieves 99.63% accuracy.

This is an open access article under the CC BY-SA license.

Corresponding Author:

Shenbagarajan Anantharajan
Department of Artificial Intelligence and Data Science, Mepco Schlenk Engineering College
Mepco Schlenk Engineering College Post, Sivakasi, Virudhunagar District, Tamil Nadu, India
Email: asrme2008@gmail.com

1. INTRODUCTION

Blood is important for life. Leukemia is a continuing problem with the blood that happens often. The amount of leukemia cases is influenced by the type of disease and the people who have it [1]. Leukemia, lymphoma, and myeloma are the main blood cancers. Leukemia starts in the bone marrow, causing it to produce many more abnormal white blood cells than usual, so the normal ones are pushed aside. Cancer symptoms usually include being tired, getting infections often, losing weight unexplained, getting bruises easily, having night sweats, and pain in the bones. Spotting blood cancer early is very important for its treatment and outlook [2]. Developments in molecular biology and personalized medicine are helping to find out more about blood cancers and create new treatments with less risk of side effects [3]. Peripheral blood smears (PBS) help find blood cancers. Since there is a lot of information and many blood cancer types, manual analysis may be slow and can lead to errors. Even though PBS uses non-ionizing radiation, the images it produces are of very high quality. Automated classification is necessary to spot dangerous blood malignancies in the early stages. After two-dimensional convolutional neural networks (CNNs) became popular, three-dimensional CNNs were adopted. A deep CNN can also be used to identify blood cancer [4]. Deep learning technology is being noticed more in medicine for its ability to accurately find and sort out different diseases. Customized deep learning-based systems for

computer-aided diagnosis (CAD) have been designed to identify leukemia from images as deep learning technology has advanced [5]. Dharani *et al.* [6] reported an improved machine-learning algorithm for blood cancer detection.

The current research is centered on developing a hybrid scheme that can segment and classify blood cancer stages through images taken by histopathology. The approach does not utilize traditional methods but uses a swin U-net transformer (UNETR) model for segmentation that takes advantage of the transformer architecture to increase the accuracy of cancer detection. Additionally, the use of local binary patterns (LBP) and adaptive threshold directional binary gradient (AT-DBGM) leads to the emergence of a novel approach for extracting low-level and high-level contextual information. Such features are useful in improving the performance of the classifier in different situations. Finally, the usage of an XGBoost classifier that has been pre-trained increases the accuracy and reliability of multi-stage blood cancer classification.

The current paper is structured to provide a clear description of the proposed approach to blood cancer segmentation and classification. Related work is presented in section 2, while section 3 defines the proposed work. Experimental details and results along with their comparison are stated in section 4. Finally, section 5 concludes the paper.

2. LITERATURE SURVEY

Ikechukwu and Murali [7] proposed i-Net, a deep CNN for white blood cancer segmentation and classification. SN-AM and acute lymphoblastic leukemia image database (ALL-IDB). The approach consisted of using the two main classification models, namely ResNet50 and VGG19 models, with the updating of their weights and parameters by transfer learning instead of using just pre-trained weights. A U-Net architecture combined with InceptionV2 was used for the segmentation stage to accurately separate leukemic cells from the blood smear images provided in the microscopic stage. These features extracted from the segmented images were then processed using a CNN to enhance the overall accuracy of the acute lymphoblastic leukemia (ALL)-detection system. The i-Net method was introduced which has extra convolutional layers and optimized values for its parameters, to separate normal from cancerous white blood cells. After 30 training cycles (epochs), the model (i-Net) accuracy started to decrease when it was not stopped early [7]. Rahman *et al.* [8] proposed to gather the data, use pre-trained CNNs to identify features in blood cell images, and then classify them with regular classifiers. The data is initially sorted into benign and malignant groups and then it is organized into four main classes. Initially, the CNN helps identify features in the images, and then the identified features are sent for feature selection with principal component analysis (PCA), linear discriminant analysis (LDA), support vector classifier (SVC), particle swarm optimization (PSO), and cat swarm optimization (CSO) [8].

Sharma *et al*. [9] proposed techniques to separate blood cell nuclei: k-means, fuzzy C-means (FCM), and k-means with firefly algorithm (FFA). Try to find the most accurate way to take out the nuclei of blood cells for use in the leukemia classification model. This study used a CNN to classify leukemia cancer by studying the microscopic images. The CNN is tested on the ALL-IDB dataset to see how accurate it is and how it measures up to the top results [9]. Ghaderzadeh *et al*. [10] provided a public dataset. Color thresholding was applied to the HSV color space using a two-channel network and then 10 famous CNN models were used to extract features from every data class. DenseNet201 was the top performer for both diagnosis and classification tasks in the 10 models. A model was finally made and offered using the most advanced technology [10]. Ahad *et al*. [11] recommend using deep CNNs that are made up of basic CNNs and those improved by transfer learning and then merged into groups to identify several types of blood cancer with very high accuracy.

A new approach is suggested that uses deep learning and machine learning techniques to automate the segmentation and classification of blood cancer. The first step in the pipeline is to resize, normalize, and use contrast-limited adaptive histogram equalization (CLAHE) on histopathological images to improve their quality and make important cellular structures more noticeable. After that, these better images are sent to the swin UNETR model, which uses transformers to accurately identify cancer-affected regions with the help of attention mechanisms. After segmenting the outputs, the hybrid method uses LBP for texture analysis and AT-DBGM for finding spatial and contextual relationships. The features are fused to form a good representation, which serves as input for the XGBoost classifier.

3. PROPOSED METHOD

The framework suggests a practical process for segmenting and classifying blood cancer using a combination of deep learning and machine learning. To begin, the histopathological images from the database are sorted into training and testing sets. Every image is preprocessed by resizing, normalizing, and using CLAHE to increase contrast and help features stand out. After preprocessing, the images are sent to the

swin UNETR model, which uses transformers to precisely separate cancerous areas. In order to extract features, a hybrid method is used that combines LBP with AT-DBGM which helps capture both local texture and the relationships between different parts of the image. After extracting features, they are combined to improve the representation and then an XGBoost classifier trained on labeled data classifies the data. In the testing phase, the data is preprocessed and segmented and features are extracted just like in training and these features are then used as input for the XGBoost model. The classifier outputs one of four possible stages: benign, early, proliferative (pro), or pre-leukemic (pre). Figure 1 illustrates the block diagram of the proposed method.

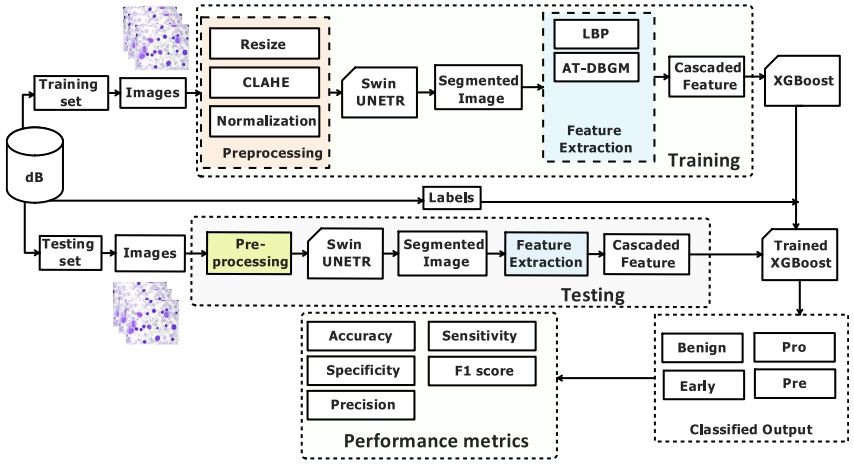

Figure 1. Block diagram of proposed method

3.1. Image resizing

This stage is important since deep neural networks need inputs of a fixed size [12], [13]. In this research, all the images were resized to 256 × 256 pixels to keep consistency within the entire dataset. Resizing decreases the computational complexity and preserves the structural data. Therefore, the model undergoes stable training and performance during segmentation and classification.

3.2. Image normalization

Z-score does not have a minimum and maximum value defined, unlike normalized values [14]–[16]. This is a technique that can be used for normalization when the range of data is unknown. It should be calculated using its mean and standard deviation [17] as shown in (1).

$$p_{normalized} = \frac{p-\mu}{\sigma} \quad (1)$$

3.3. Contrast limited adaptive histogram equalization

CLAHE is a method used to enhance the contrast of medical images through the distribution of the pixel intensity values. The steps involved in the CLAHE algorithm include splitting the input image into non-overlapping tiles and equalizing the histograms in each tile separately [18]. Mathematically, the transformation function $T(r)$ of the pixel intensity value r in a tile is defined as (2).

$$T(r) = \frac{(C(r)-C_{min})}{(M\times N-C_{min})} \times (L-1) \quad (2)$$

3.4. Swin U-net transformer

Swin UNETR captures both global and local contextual features efficiently while preserving spatial details through skip connections [19]. Given an input CT scan image, X of size $H \times W \times C$, swin UNETR first divides it into non-overlapping patches, as formulated in (3).

$$z_0 = [X_p^1 E;\ X_p^2 E; \ldots . X_p^N E + E_{POS} \quad (3)$$

Where X_p^i is the ith image patch. E is the learnable embedding matrix, E_{POS} is the positional encoding to retain spatial information. Each patch representation is fed into the swin transformer encoder for hierarchical feature extraction (4) and (5).

$$\mathrm{Q} = \mathrm{ZW_Q}, \mathrm{K} = \mathrm{ZW}_K, \mathrm{V} = \mathrm{ZW}_v \tag{4}$$

$$\mathrm{Attention}(\mathrm{Q}, \mathrm{K}, \mathrm{V}) = \mathrm{softmax}\left(\frac{\mathrm{QK}^T}{\sqrt{d_k}}\right)\mathrm{V} \tag{5}$$

Where $\mathrm{W_Q}$, W_K, W_v are learnable weight matrix. d_k is the dimension of keys. The hierarchical encoder produces multi-scale feature maps $\{Z1, Z2, Z3, Z4\}$ is defined in (6) and (7).

$$\{Z_1, Z_2, Z_3, Z_4\} \tag{6}$$

$$X_{\mathbf{skip}} = \mathrm{Concat}(Z_i, \mathrm{X_{up}}) \tag{7}$$

Where Z_i is the feature map from the encoder. $\mathrm{X_{up}}$ is the upsampled decoder feature map. A convolutional layer then refines the features is defined in (8).

$$X_{\mathrm{final}} = \sigma(W_{conv}, * X_{\mathbf{skip}} + \mathrm{b}_{conv}) \tag{8}$$

$$\mathrm{Y} = \sigma(W_{\mathrm{out}}, * X_{\mathrm{final}} + \mathrm{b_{out}}) \tag{9}$$

Where W_{out} the output weight matrix, σ is a softmax or sigmoid activation function, and Y represents the predicted liver tumor segmentation mask as shown (9).

Table 1 presents the parameter specifications of the proposed swin UNETR-based segmentation model. A batch size of 16 balances computational efficiency and performance, while layer normalization stabilizes training. The swin transformer uses a 4 × 4 patch size to capture hierarchical spatial features.

Table1. Parameter specification of swin UNETR

Parameter	Value
Batch size	16
Epochs	125
Activation function	Sigmoid
Patch size	4 × 4
Loss function	Dice loss
Optimizer	AdamW
Learning rate scheduler	Cosine annealing
Learning rate	1e-4

3.5. Adaptive threshold directional binary gradient matrix

Using the AT-DBGM can give a clearer and more detailed view of binary data, which might lead to better performance in machine learning models. At every pixel (i, j) in the binary matrix B, the local gradient direction is calculated as presented in (10) to (17).

$$S_x = \begin{bmatrix} -1 & 0 & 1 \\ -2 & 0 & 2 \\ -1 & 0 & 1 \end{bmatrix} \tag{10}$$

$$S_y = \begin{bmatrix} -1 & -2 & -1 \\ 0 & 0 & 0 \\ 1 & 2 & 1 \end{bmatrix} \tag{11}$$

$$G_x(i, j) = \sum_{m=-1}^{1} \sum_{n=-1}^{1} S_x(m, n).\, \mathrm{B(i + m, j + n)} \tag{12}$$

$$G_y(i, j) = \sum_{m=-1}^{1} \sum_{n=-1}^{1} S_y(m, n).\, \mathrm{B(i + m, j + n)} \tag{13}$$

$$\mathrm{g(i, j)} = \sqrt{G_x(i, j)^2 + G_y(i, j)^2} \tag{14}$$

$$\theta\mathrm{(i, j)} = \arctan\left(\frac{G_y(i,j)}{G_x(i,j)}\right) \tag{15}$$

$$\Theta_k = \left[\theta_k, \theta_k + \frac{\pi}{K}\right), K = 1,2, \ldots . K \tag{16}$$

$$\mathrm{D(i, j)} = \frac{1}{|\mathrm{W(i,j)}|} \sum_{(m,n) \in W(i,j)} \mathrm{B(m, n)} \tag{17}$$

The window size $|\ W(i, j)\ |$ is set such that as expressed in (18).

$$\mathrm{W(i,j)} \mid= \min\left(\max\left(\alpha.\frac{1}{\mathrm{D(i,j)}}, W_{min}\right), W_{max}\right) \quad (18)$$

For each direction bin k, the binary directional co-occurrence matrix Mk is computed as (19).

$$M_k(i,j) = \sum_{(m,n)\in W(i,j)} 1_{\{B(i,j)=1\}}.\, 1_{\{B(m,n)=1\}}\, 1_{\{\theta(i,j)=\Theta_k\}}.\, 1_{\{\theta(m,n)=\Theta_k\}} \quad (19)$$

Where $1\{\cdot\}$ is indicator function. The AT-DBGM is aggregated across all directional bins k as given in (20).

$$\mathrm{AT-DBGM} = \sum_{k=1}^{K} M_k \quad (20)$$

The directional entropy Ek is computed for each bin k as defined in (21) and (22).

$$E_k = -\sum_{i,j} M_k(\mathrm{i,j}) \log M_k(\mathrm{i,j}) \quad (21)$$

$$E_k = \sum_{k=1}^{K} M_k \quad (22)$$

The AT-DBGM is computed at multiple scales by varying the resolution of the binary matrix B. For scale s, let $B(s)$ denote the matrix at scale s as indicated in (23).

$$B^{(S)}\mathrm{Resize(B, scale = s)} \quad (23)$$

AT-DBGM is computed for each scale s, denoted AT-DBGM$^{(s)}$.The multi-scale consistency $C(s1, s2)$ between scales $s1$ and $s2$ as formulated in (24).

$$C(S_1, S_2) = \frac{1}{|\mathrm{AT-DBGM}^{(S_1)}|.|\mathrm{AT-DBGM}^{(S_2)}|} \sum_{i,j} \mathrm{AT-DBGM}^{(S_1)}(\mathrm{i,j}) \cdot \mathrm{AT-DBGM}^{(S_2)}(\mathrm{i,j}) \quad (24)$$

The final feature vector F is constructed by concatenating the extracted features as given in (25).

$$F = [Etotal, C(s1, s2), Contrast, Correlation, Energy, Homogeneity, \dots] \quad (25)$$

Where contrast, correlation, energy, and homogeneity are computed using the traditional gray-level co-occurrence matrix (GLCM) definitions but applied to the $\mathrm{AT-DBGM}$.

3.6. Local binary pattern

LBP is found to be very useful and efficient in the field of texture analysis, and it is particularly suited for real-time applications due to less consumption of computing power [20]. In the LBP feature, the binary number is generated from the difference in intensity of the center pixel and the neighboring pixels as presented in (26) and (27).

$$LBP_{p,r} = \sum_{r=0}^{p-1} s(G_p - G_c) 2^p \quad (26)$$

$$S_x = \begin{cases} 1, & if\ x \geq 0 \\ 0, & if\ x < 0 \end{cases} \quad (27)$$

3.7. XGBoost

XGBoost is a tree-based ensemble classification learning method that gained popularity and is widely used in the area of classification due to its high computational efficiency, high scalability, and high prediction accuracy [21]. In this work, DenseNet201's traditional fully connected layer (FCL) is replaced by an XGBoost classifier to boost the final classification result. XGBoost builds an ensemble of decision trees by an additive boosting method, each tree is trained to reduce the errors that the previous trees made. The algorithm optimizes the objective function iteratively to obtain a strong and accurate classification model, having n samples and m input features as expressed in (28) to (32).

$$\hat{y}_i = \sum_{k=1}^{K} f_k(x_i) \qquad f_k \in \mathrm{F} \quad (28)$$

$$\mathrm{L} = \sum_{k=1}^{K} L(y_i, \hat{y}) + \sum_{k=1}^{K} \Omega(f_k) \quad (29)$$

$$\Omega(\mathrm{f}) = \gamma \mathrm{T} + \frac{1}{2}\lambda \sum_{J=1}^{T} w_j^2 \quad (30)$$

$$L^{(t)} \approx \sum_{i=1}^{n}\left[g_i f(x_i) + \frac{1}{2} h_i f^2(x_i)\right] + \Omega(\mathrm{f}) \quad (31)$$

$$\text{Gain} = \frac{1}{2}\left[\frac{(\Sigma g_{L,})^2}{\Sigma h_{L,}+\lambda} + \frac{(\Sigma g_{R,})^2}{\Sigma h_{R,}+\lambda} - \frac{(\Sigma g)^2}{\Sigma h+\lambda}\right] - \gamma \quad (32)$$

XGBoost's efficiency is further improved by column subsampling, tree pruning, and parallel processing, making it one of the most powerful algorithms for structured data classification tasks. Table 2 summarizes the key hyperparameters used to train the XGBoost classifier in the blood cancer classification framework.

Table 2. Training parameters of XGBoost

Parameter	Typical values
max_depth	5
Lambda	8
Objective	binary
tree_method	hist
learning_rate	0.02
min_child_weight	6
Booster	gbtree
Gamma	5

4. RESULTS AND DISCUSSIONS

To evaluate the proposed methods, this study used the PyTorch 6 framework in Python 3.6, which made sure the deep learning models ran smoothly. The experiments were conducted on a PC equipped with 16 GB of RAM, Intel Core i7-4790 processor at 3.60 GHz and an NVIDIA TITAN X GPU. The architecture of this hardware enabled faster training and inference, helping to efficiently manage large medical images.

4.1. Dataset

ALL detection can be done through invasive, expensive, and time-consuming tests [22]. The dataset contains 3,256 images of PBS, taken from 89 suspected ALL patients from Taleqani Hospital in Tehran, Iran. These images were prepared and stained to categorize whether they are benign (hematogones) or malignant. These images were taken using a Zeiss microscope at 100× magnification in JPG form and verified by flow cytometry. HSV color-thresholding images were also acquired. Dataset information is provided in Table 3 and image samples are illustrated in Figure 2. The dataset consists of four representative cell categories, including benign as in Figure 2(a), early as in Figure 2(b), pre-leukemic as in Figure 2(c), and proliferative as in Figure 2(d).

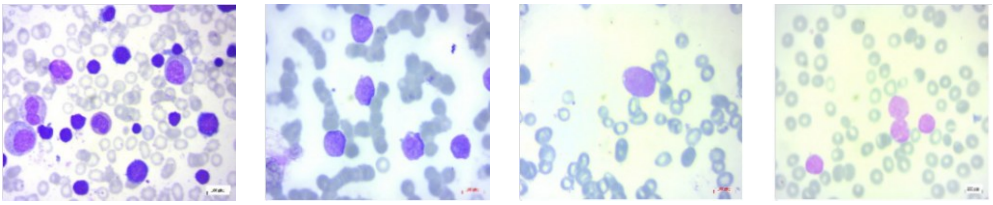

(a) (b) (c) (d)

Figure 2. Sample images from the dataset: (a) benign, (b) early, (c) pre-leukemic, and (d) proliferative

Table 3. The training, test, and validation involved the use of a distribution of PBS images

Class	No of images	Training images	Validation images
Benign	505	354	100
Pre-leukemic-B	955	669	190
Early Pre-B	979	687	193
Proliferative-B	796	558	158
Total	3235	2268	641

Performance metrics help to numerically measure the efficiency and reliability of the classification model. Accuracy [23], precision [24], recall [25], and the F1-score and specificity are some of the measures that provide complementary information on the performance of the classification model as formulated in (34) to (43).

$$\text{DSC} = \frac{2\text{TP}}{\text{FP} + 2\text{TP} + \text{FN}} \tag{34}$$

$$VOE = 1 - \frac{|A \cap B|}{|A \cup B|} \tag{35}$$

$$MSD(A,B) = \frac{1}{|A|}\sum_{a \in A} \min_{b \in B} d(a,b) \tag{36}$$

$$IoU = \frac{|A \cap B|}{|A \cup B|} \tag{37}$$

$$HD(A,B) = max(\sup_{a \in A} inf_{b \in B}\, d(a,b), \sup_{b \in B} inf_{b \in A}\, d(a,b)) \tag{38}$$

$$\text{Accuracy} = \frac{\text{TP+TN}}{\text{TP+TN} + \text{FP+FN}} \tag{39}$$

$$\text{Precision} = \frac{\text{TP}}{\text{TP} + \text{FP}} \tag{40}$$

$$\text{Recall} = \frac{\text{TP}}{\text{TP} + \text{FN}} \tag{41}$$

$$\text{F1} - \text{score} = \frac{2*(\text{Recall}*\text{Precision})}{\text{Recall+Precision}} \tag{42}$$

$$\text{Specificity} = \frac{\text{TN}}{\text{TN} + \text{FP}} \tag{43}$$

Figure 3 illustrates the segmented image of the sample. Table 4 gives a comparative analysis of segmentation performance metrics used to assess the effect of employing CLAHE during the preprocessing phase. From the results, it is clear that the integration of CLAHE greatly boosts the efficiency of segmentation. The Dice similarity coefficient (DSC) increased from 94.82% to 97.36%, which implies that the predicted and ground truths have high overlap. Likewise, the mean surface distance (MSD) decreased from 1.91 px to 1.23 px, and the Hausdorff distance (HD) decreased from 6.54 px to 4.17 px, meaning that the boundary prediction was highly precise. In addition, the volume overlap error (VOE) decreased from 8.45% to 5.72%, and the intersection over union (IoU) increased from 90.12% to 94.86%.

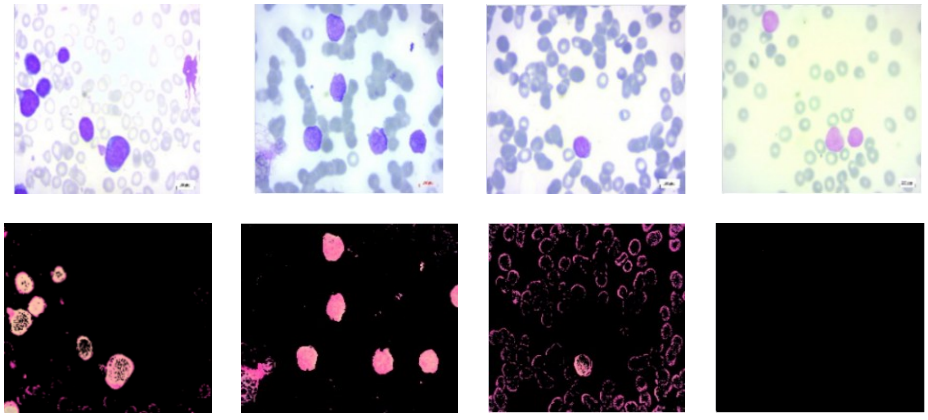

Figure 3. Sample segmented image

Table 4. Segmentation performance comparison

Metric	Without CLAHE	With CLAHE
DSC (%)	94.82	97.36
MSD (px)	1.91	1.23
VOE (%)	8.45	5.72
IoU (%)	90.12	94.86
HD (px)	6.54	4.17

Table 5 provides an overview of the effects of CLAHE and AT-DBGM on model performance with respect to the three configurations considered. The application of CLAHE and AT-DBGM produces the most effective results, delivering the highest accuracy (99.63%), precision (99.46%), recall (99.98%), F1-score (99.85%), and specificity (99.09%) among the models. Table 6 shows the effect of various training and testing ratios on the performance of the proposed blood cancer classification model.

Table 5. Performance of classification based on CLAHE and AT-DBGM

Performance	Without CLAHE	Without AT-DBGM	CLAHE + AT-DBGM
Accuracy	99.18	98.43	99.63
Precision	99.30	98.28	99.46
Recall	99.18	98.32	99.98
F1- score	99.19	98.30	99.85
Specificity	98.54	98.06	99.09

Table 6. Performance at different training and testing ratios

Train : test ratio	Accuracy (%)	Precision (%)	Recall (%)	F1-score (%)	Specificity (%)
40 : 60	55.63	52.19	51.36	48.64	51.79
45 : 55	58.31	60.13	55.28	53.67	59.47
50 : 50	62.36	64.39	62.51	56.43	63.48
55 : 45	76.97	79.94	68.47	66.41	69.21
60 : 40	81.85	83.15	76.58	69.58	75.64
65 : 35	88.69	84.96	86.48	89.64	81.69
70 : 30	98.96	98.62	99.12	98.87	98.55
80 : 20	99.63	99.46	99.98	99.85	99.09

Table 7 shows that the proposed method is better than i-Net, ResNet50, VGG-16, and SVM since it has the best performance in terms of all the criteria mentioned. In particular, the proposed method produces the best accuracy score (99.63%) as compared to i-Net (99.18%), ResNet50 (98.43%), VGG-16 (90.1%), and SVM (83.33%). Also, the proposed method has the best precision (99.46%) rates.

Table 7 Comparative performance of the proposed method

Performance	i-Net [6]	ResNet50 [7]	SVM [11]	VGG-16 [12]	This work
Accuracy	99.18	98.43	83.33	90.1	99.63
Precision	99.30	98.28	84.56	84.88	99.46
Recall	99.18	98.32	88.94	93.58	99.98
F1-score	99.19	98.30	90.41	89.01	99.85
Specificity	98.54	98.06	88.43	87.5	99.09

5. CONCLUSION

In this paper, a new and efficient method of detecting and classifying blood cancer has been introduced, combining the high-quality segmentation capabilities of the swin UNETR model with feature extraction techniques and the effective XGBoost classifier. The use of preprocessing techniques (CLAHE) and hybrid feature extraction with LBP and AT-DBGM allows obtaining both local texture features and context features from the images. The cascading feature representation allows improving the classification performance and achieving a good result for classifying blood cancer stages (benign, early, proliferate, pre-leukemic). The proposed technique achieved excellent results in terms of accuracy (99.63%), precision (99.46%), recall (99.98%), F1-score (99.85%), and specificity (99.09%). Generally, the method has great potential in real time diagnostics, leading to early diagnosis, effective treatment, and good clinical results in blood cancer diagnosis.

FUNDING INFORMATION

Authors state no funding involved.

AUTHOR CONTRIBUTIONS STATEMENT

This journal uses the Contributor Roles Taxonomy (CRediT) to recognize individual author contributions, reduce authorship disputes, and facilitate collaboration.

Name of Author	C	M	So	Va	Fo	I	R	D	O	E	Vi	Su	P	Fu
Shenbagarajan Anantharajan	✓	✓							✓		✓			
Shenbagalakshmi Gunasekaran		✓						✓	✓					
Sivaganesh Anantharajan	✓					✓				✓				
Thavasi Subramanian	✓				✓					✓		✓	✓	

C : **C**onceptualization
M : **M**ethodology
So : **So**ftware
Va : **Va**lidation
Fo : **Fo**rmal analysis
I : **I**nvestigation
R : **R**esources
D : **D**ata Curation
O : Writing - **O**riginal Draft
E : Writing - Review & **E**diting
Vi : **Vi**sualization
Su : **Su**pervision
P : **P**roject administration
Fu : **Fu**nding acquisition

CONFLICT OF INTEREST STATEMENT

Authors state no conflict of interest.

DATA AVAILABILITY

The original data can be accessed at https://www.kaggle.com/datasets/mehradaria/leukemia.

REFERENCES

[1] M. E. Billah and F. Javed, "Bayesian convolutional neural network-based models for diagnosis of blood cancer," *Applied Artificial Intelligence*, vol. 36, no. 1, 2022, doi: 10.1080/08839514.2021.2011688.

[2] E. A. Alabdulqader *et al.*, "Improving prediction of blood cancer using leukemia microarray gene data and Chi2 features with weighted convolutional neural network," *Scientific Reports*, vol. 14, no. 1, 2024, doi: 10.1038/s41598-024-65315-7.

[3] Q. Zhao, Y. Cao, and W. Luo, "Blood cancer detection based on CNN and integrated learning," in *2025 5th International Conference on Computer Vision, Application and Algorithm, CVAA 2025*, 2025, doi: 10.1109/CVAA66438.2025.11193260.

[4] J. B. Awotunde *et al.*, "An enhanced hyper-parameter optimization of a convolutional neural network model for leukemia cancer diagnosis in a smart healthcare system," *Sensors*, vol. 22, no. 24, 2022, doi: 10.3390/s22249689.

[5] P. K. Das and S. Meher, "An efficient deep convolutional neural network based detection and classification of acute lymphoblastic leukemia," *Expert Systems with Applications*, vol. 183, 2021, doi: 10.1016/j.eswa.2021.115311.

[6] N. P. Dharani, G. Sujatha, and R. Rani, "Blood cancer detection using improved machine learning algorithm," in *2023 International Conference on Circuit Power and Computing Technologies, ICCPCT 2023*, 2023, pp. 1136–1141, doi: 10.1109/ICCPCT58313.2023.10245375.

[7] A. V. Ikechukwu and S. Murali, "i-Net: a deep CNN model for white blood cancer segmentation and classification," *International Journal of Advanced Technology and Engineering Exploration*, vol. 9, no. 95, 2022, doi: 10.19101/IJATEE.2021.875564.

[8] W. Rahman, M. G. G. Faruque, K. Roksana, A. H. M. S. Sadi, M. M. Rahman, and M. M. Azad, "Multiclass blood cancer classification using deep CNN with optimized features," *Array*, vol. 18, 2023, doi: 10.1016/j.array.2023.100292.

[9] A. Sharma, D. Prashar, A. A. Khan, F. A. Khan, and S. Poochaya, "Automatic leukaemia segmentation approach for blood cancer classification using microscopic images," *Computers, Materials and Continua*, vol. 73, no. 2, pp. 3629–3648, 2022, doi: 10.32604/cmc.2022.030879.

[10] M. Ghaderzadeh, M. Aria, A. Hosseini, F. Asadi, D. Bashash, and H. Abolghasemi, "A fast and efficient CNN model for B-ALL diagnosis and its subtypes classification using peripheral blood smear images," *International Journal of Intelligent Systems*, vol. 37, no. 8, pp. 5113–5133, 2022, doi: 10.1002/int.22753.

[11] M. T. Ahad, I. J. Payel, B. Song, and Y. Li, "DVS: blood cancer detection using novel CNN-based ensemble approach," 2024, *arXiv:2410.05272*.

[12] P. Sachin and K. Yogesh, "Detection and classification of blood cancer from microscopic cell images using SVM KNN and NN classifier," *International Journal of Advance Research, Ideas and Innovations in Technology*, vol. 3, no. 6, pp. 315–324, 2007.

[13] D. Kumar *et al.*, "Automatic detection of white blood cancer from bone marrow microscopic images using convolutional neural networks," *IEEE Access*, vol. 8, pp. 142521–142531, 2020, doi: 10.1109/ACCESS.2020.3012292.

[14] C. Ananth, M. Sridharan, and S. A. James, "An advanced low-cost blood cancer detection system," *International Journal of Early Childhood Special Education*, vol. 14, no. 5, 2022, doi: 10.9756/INTJECSE/V14I5.475.

[15] N. Saranyan, N. Kanthimathi, P. Ramya, N. Kowsalya, and S. Mohanapriya, "Blood cancer detection using machine learning," in *2021 5th International Conference on Electronics, Communication and Aerospace Technology, ICECA 2021*, 2021, pp. 1–11, doi: 10.1109/ICECA52323.2021.9675987.

[16] C. Ananth, P. Tamilselvi, S. A. Joshy, and T. A. Kumar, "Blood cancer detection with microscopic images using machine learning," in *Machine Learning in Information and Communication Technology*, Singapore: Springer, 2022, pp. 45–54, doi: 10.1007/978-981-19-5090-2_4.

[17] P. K. Das, B. Nayak, and S. Meher, "A lightweight deep learning system for automatic detection of blood cancer," *Measurement: Journal of the International Measurement Confederation*, vol. 191, 2022, doi: 10.1016/j.measurement.2022.110762.

[18] M. Bukhari, S. Yasmin, S. Sammad, and A. A. A. El-Latif, "A deep learning framework for leukemia cancer detection in microscopic blood samples using squeeze and excitation learning," *Mathematical Problems in Engineering*, vol. 2022, 2022, doi: 10.1155/2022/2801227.

[19] F. M. Talaat and S. A. Gamel, "A2M-LEUK: attention-augmented algorithm for blood cancer detection in children," *Neural Computing and Applications*, vol. 35, no. 24, pp. 18059–18071, 2023, doi: 10.1007/s00521-023-08678-8.

[20] S. Selvakumaran, C. Poonguzhali, E. Baskaran, A. Arya, D. K. Nayak, and S. Gupta, "Integrated hybrid deep learning approach for precise blood cancer detection," in *2024 10th International Conference on Communication and Signal Processing, ICCSP 2024*, 2024, pp. 496–501. doi: 10.1109/ICCSP60870.2024.10544027.
[21] C. Spandana and R. P. Kumar, "Detection of cancer in human blood sample using machine learning," in *7th International Conference on Computing Methodologies and Communication, ICCMC 2023*, 2023, pp. 197–204. doi: 10.1109/ICCMC56507.2023.10083971.
[22] A. I. Shehta, M. Nasr, and A. E. D. M. El Ghazali, "Blood cancer prediction model based on deep learning technique," *Scientific Reports*, vol. 15, no. 1, 2025, doi: 10.1038/s41598-024-84475-0.
[23] W. Rösler, M. Roiss, and C. Widmer, "Advancements in machine learning (ML): transforming the future of blood cancer detection and outcome prediction," *Healthbook TIMES Oncology Hematology*, vol. 20, no. 2, pp. 20–25, 2024, doi: 10.36000/HBT.OH.2024.20.146.
[24] H. Mohamed, F. K. Elsheref, and S. R. Kamal, "A new model for blood cancer classification based on deep learning techniques," *International Journal of Advanced Computer Science and Applications*, vol. 14, no. 6, pp. 422–429, 2023, doi: 10.14569/IJACSA.2023.0140645.
[25] A. K. Sharma and M. Mandot, "Modified method of diagnosis of blood cancer using MRI classification through machine learning image acquisition - image pre-processing nucleus segmentation," *Turkish Journal of Computer and Mathematics Education*, vol. 12, no. 10, pp. 3509–3513, 2021.

BIOGRAPHIES OF AUTHORS



Shenbagarajan Anantharajan is an associate professor in the Department of Artificial Intelligence and Data Science at Mepco Schlenk Engineering College, Sivakasi. He earned his B.E. in Electrical and Electronics Engineering from P.S.R. Engineering College, Sivakasi, and his M.E. in Computer Science and Engineering from National Engineering College, Kovilpatti, both affiliated with Anna University, Chennai. He completed his Ph.D. in Computer Science and Engineering at Annamalai University, Chidambaram. With over 15 years of teaching experience and 2 years in industry, he has presented 45 papers in national and international journals and symposiums. His research interests include artificial intelligence, network security, internet of things, and soft computing. He can be contacted at email: shenbagarajan@mepcoeng.ac.in.



Shenbagalakshmi Gunasekaran is an assistant professor (senior) in the Department of Computer Science and Engineering at Mepco Schlenk Engineering College, Sivakasi. She earned her B.Tech. in Information Technology from Arulmigu Kalasalingam Engineering College, Srivilliputhur; and her M.E. in Computer Science and Engineering from Mepco Schlenk Engineering College, both affiliated with Anna University, Chennai. She completed her Ph.D. in Computer Science and Engineering at Anna University, Chennai. With over 5 years of teaching experience and 5 years of research experience, she has presented 23 papers in national and international journals and symposiums. Her research interests include wireless sensor networks, internet of things, and soft computing. She can be contacted at email: pri.infotech@gmail.com or shenbagalakshmi@mepcoeng.ac.in.



Sivaganesh Anantharajan is working as an assistant professor in the Master of Computer Application at Mepco Schlenk Engineering College, Sivakasi. He graduated in Bachelor of Engineering in Electronics and Communication Engineering at P. S. R. Engineering College, Sivakasi, affiliated to Anna University, Chennai, Tamil Nadu, India. He secured a Master of Engineering in Computer Science and Engineering at SRM University, Chennai, and Tamilnadu, India. He is in the teaching profession for more than 6 years. He has presented 3 papers in national and international journals, conferences, and symposiums. His main areas of interest include image processing, internet of things, and soft computing. He can be contacted at email: psasivaganesh@gmail.com.



Thavasi Subramanian is an assistant professor (selection grade) in the Department of Computer Science and Engineering at Mepco Schlenk Engineering College, Sivakasi. He earned his B.E. in Computer Science and Engineering from Mepco Schlenk Engineering College, Sivakasi, and his M.E. in Computer Science and Engineering from Madras Institute of Technology, Chennai, both affiliated with Anna University, Chennai. He is currently pursuing his Ph.D. in Computer Science and Engineering at Anna University, Chennai. With over 13 years of teaching experience, he has presented 11 papers in national and international journals and symposiums. His research interests include text mining, data mining, and soft computing. He can be contacted at email: sktthavasi@gmail.com or sktthavasi@mepcoeng.ac.in.